Malaysian Journal of Catalysis

http://mjcat.utm.my/

MJCat

Research Article

Photodegradation of Methylene Blue and Methyl Orange using Metal Oxide Photocatalysts

Ray Georgeny[1] and Rohul Adnan[1,2]*

[1] Department of Chemistry, Faculty of Science, Universiti Teknologi Malaysia, 81310 UTM Johor Bahru, Johor, Malaysia.
[2] Center for Hydrogen Energy, Institute for Future Energy, Universiti Teknologi Malaysia, 81310 UTM Johor Bahru, Johor, Malaysia

Corresponding Author: rohulhayat@utm.my

GRAPHICAL ABSTRACT

ABSTRACT

Dyes are important in textile, food and cosmetic industry. Unfortunately, some dyes are highly toxic even in the presence of a tiny amount. Photocatalyst is a catalyst that drives chemical reactions under light irradiation and produces a strong oxidizing agent to treat the dye. There are several factors that affect the rate of degradation of dye such as the pH, type and amount of photocatalyst and concentration of dye. Out of all metal oxides used in this study, nickel ferrite ($NiFe_2O_4$) and zinc ferrite ($ZnFe_2O_4$) are catalytically inert while zinc oxide (ZnO) and titanium dioxide (TiO_2) are photocatalytically active and thus used in the subsequent studies. Photodegradation of methylene blue (MB) and methyl orange (MO) using ZnO and TiO_2 was taken at 90 minutes to show the effect of pH. At pH 5, TiO_2 and ZnO showed 67% and 97%, and at pH 9, both photocatalyst have 97% photodegradation rate of MB, respectively. For photodegradation of MO, at pH 5 both photocatalysts have similar photodegradation rate. At pH 9, TiO_2 and ZnO has a 78% and 95% photodegradation rate of MO. The rate of was found to increase proportionally with the amount of photocatalyst used but at high concentration, the degradation rate was saturated. The optimized condition for photodegradation of MB is at pH 9 and MO at pH 5 using 30 mg photocatalysts (ZnO or TiO_2) owing to the cationic and anionic character of the dyes. The crystal structure of TiO_2 and ZnO are tetragonal anatase and hexagonal wurtzite, respectively, as verified by XRD. FESEM images revealed that ZnO consists of nanoparticles and nanoplatelets with average size of 45.5 ± 14.1 nm and TiO_2 shows average size of 42.5 ± 10.5 nm. The band gap of TiO_2 and ZnO are 3.46 and 3.26 eV, respectively, as calculated from the UV-visible diffuse reflectance spectroscopy (UV-vis DRS). The X-ray photoelectron spectra for TiO_2 confirm the presence of Ti^{4+} and O^{2-} states.

Keywords: photocatalysts, methylene blue, methyl orange, metal oxides

1. INTRODUCTION

Photocatalytic technology is a viable and green approach for degradation of organic dyes, photoreduction of CO_2 and photocatalytic water splitting. Metal oxide semiconductors are suitable photocatalysts due to their high photosensitivity, stability, low cost and suitable band gap [1]. Photoexcited electrons play a role in reduction processes whereas photogenerated holes in oxidation processes. Upon light irradiation, these photogenerated charge carriers create radical species ($\cdot OH^-$, $\cdot O_2^-$) that are responsible for degradation of dyes. Photodegradation of dyes is useful for water treatment process to discharge dye pollutants [2].

Commonly used dyes in photocatalytic studies are methylene blue (MB) and methyl orange (MO).

Suitable morphology, high surface area, narrow band gap, stability, and low recombination rate of charge carriers are some of key features that a good photocatalyst should possess [3]. Semiconductor photocatalysts such as TiO_2 and ZnO exhibit most of those features making them desirable and commonly employed photocatalytic in a myriad of reactions. Owing to these properties, it is natural to use TiO_2 and ZnO as benchmark photocatalysts to investigate the factors affecting the photocatalytic performance.

Herein, we employ a variety of commercial metal oxides ($NiFe_2O_4$, $ZnFe_2O_4$, WO_3, TiO_2, ZnO) nanopowders to investigate the factors affecting the photocatalytic

performance in degradation of MB and MO. The optimized conditions show that the almost a complete degradation was achieved in 90 minutes.

2. EXPERIMENTS

2.1 Materials

Methyl orange (MO) and methylene blue (MB) were purchased from Across Organic. $NiFe_2O_4$ (purity 98%, APS 30 nm), $ZnFe_2O_4$ (purity 98.5%, APS 10-30 nm), TiO_2 (purity 99.9%, APS 18 nm), ZnO (purity 99+%, APS 10-30 nm) and WO_3 (purity 99.9%, APS 60 nm, tetragonal) were purchased from US Research Nanomaterials, Inc. Hydrochloric acid (HCl), sodium hydroxide (NaOH) were supplied by Merck. Reagents were of analytical grade and used without further purification.

2.2 Photocatalytic rection

A homemade photocatalytic reactor was built from closed, rectangle wood box equipped with UV lamp 365 nm, 90 W tube (VL-315 BL, Made in France). The amount of photocatalyst for this experiment was set to 10, 20 and 30 mg. The concentration of dyes (MB and MO) was varied from 10 to 30 mg/L. Briefly, the photocatalytic experiment was performed by charging a specific amount photocatalysts into a glass beaker containing dye solution. The dye solution was stirred in the dark for one hour to allow equilibrium between adsorption and desorption of dyes onto/from photocatalysts. After one hour, the UV light was switched on to initiate photocatalytic reaction. Sampling was done by taking ca. 1 mL dye solution every 30 minutes over the course of 90 minutes.

UV-visible spectroscopy was used to measure the concentration of dyes before and after photodegradation. The absorbance peak for methylene blue (MB) is at 664 nm and for methyl orange (MO) at 464 nm. The change in the absorbance intensity of at these peak maxima was monitored to quantify the change in the concentration of dyes.

2.3 Characterization

XRD patterns were collected using Rigaku SmartLab diffractometer with Cu anode at 1.5418 Å. Surface morphology and size were imaged using a FESEM Hitachi SU8020 at operating voltage 2.0 kV. The images were analyzed using ImageJ software package from at least 150 particles to construct the statistic and histogram. The band gap was determined using UV-visible spectrophotometer Shimadzu UV3600Plus Series in a reflectance mode with wavelength between 200 and 800 nm. X-ray photoelectron (XP) spectra were scanned at Synchrotron Light Research Institute (Public Organization) in Nakhon Ratchasima using a photon energy of 650 eV. The high-resolution XP spectra for Ti 2p and O 1s were recorded with energy step of 0.1 eV.

3. RESULTS AND DISCUSSION

Metal oxide nanoparticles used as photocatalysts in this study are titanium dioxide (TiO_2), zinc oxide (ZnO), tungsten trioxide (WO_3), zinc ferrite ($ZnFe_2O4$) and nickel ferrite ($NiFe_2O_4$) in photodegradation of methylene blue (MB) and methyl orange (MO). TiO_2 and ZnO showed a a significant converstion as they managed to achieve almost a complete dedegrade the dyes while the other three photocatalysts, WO_3, $ZnFe_2O_4$ and $NiFe_2O_4$ were completely inactive despite the narrow band gap (< 3.0 eV). WO_3, $ZnFe_2O_4$ and $NiFe_2O_4$ are inactive due to the fast recombination rate of electron-hole pairs [4-6]. This prevents the formation of long-lived free charge carriers (electron and hole) which are responsible for the degradation formation of hydroxyl radicals for dye degradation.

ZnO was proven to have a better efficiency than TiO_2 due to the presence of mixed nanoplates and nanoparticles in ZnO which provide a high surface area and promote a charge separation and transfer due to the interface contact between the two structures.

The rate of degradation of the dyes was studied in the pH range of between 3 and 11 to determine the optimum pH for each dye. The effects of pH in the photocatalytic degradation of MB and MO are summarized in Figure 3. The initial duration of 3 hrs for photodegradation was chosen but upon optimization it was found that 90 mins was sufficient to get very high photodegradation rate (> 90%). MB was discuss first followed by MO to have a better understanding of both dye photodegradation. Photodegradation for MB and MO at neutral conditions (pH 7) was found to be much lower that in acidic and basic conditions. $NiFe_2O_4$, $ZnFe_2O_4$ and WO_3 were found to be photocatalytically ineffective. Thus, we focus our discussion on ZnO and TiO_2 photocatalysts in acid and basic media in the following paragraphs.

For MB degradation, at pH 5 the photodegradation rate using TiO_2 was found to be at 67%. When ZnO was used, the photodegradation rate was at 97%. But surprisingly at pH 9, both photocatalysts have the same photodegradation rate at 97%. The degradation of the MB dye in TiO_2 and ZnO was found to increase as the pH increases from acidic to alkaline due to MB having a positive charge on nitrogen atom (indicates MB is a cationic dye) in the amine group of the dye. However, the pH effect did not affected ZnO photocatalysts perhaps because the point of zero charge for ZnO is 9 (compared with that of TiO_2: 6.8) [7]. The increase of pH will produce OH^- ions which cause deprotonation on the surface of both photocatalyst, resulting in better electrostatic interaction between negatively charged surface of photocatalyst and positively charged MB [8].

At pH 5 in MO photodegradation, TiO₂ and ZnO have almost the same photodegradation with 94% and 96%, respectively. However, at pH 9, TiO₂ only degraded 78% of MO when compared to ZnO, which has a photodegradation rate of 95%. the degradation of MO thrives in acidic condition due to the MO having a negative charge on oxygen atom (indicates MO is an anionic dye) in the sulfonate group of the [9]. The presence of H^+ ion will cause the surface of photocatalyst, TiO₂ and ZnO to be positively charged. This will cause MO to be adsorbed electrostatically more efficiently due to its attraction with the positively charged surface TiO₂ and ZnO. Another reason for a fast degradation of MO in acidic condition is the structural change of MO in acidic condition. The quinoid structure of MO has a relatively lower bond energy as compared to the MO azo structure. This renders MO more easily to be degraded. Figure 1 shows the effect of pH on MB and MO photodegradation rate at 90 mins.
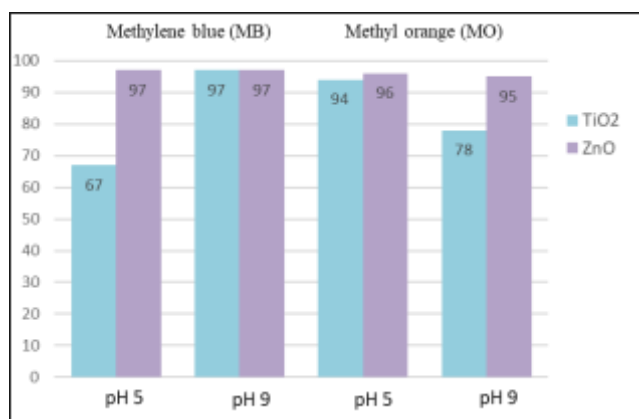

Fig. 1 Effect of pH on the photodegradation rate of MB and MO using TiO₂ and ZnO at 90 minutes

Different initial concentrations of MB from 20 ppm, 30 ppm and 40 ppm were used to evaluate the effect of concentration on the photocatalytic activity of photocatalyst. At 30 and 40 ppm, the absorbance of MB was found to be in the range higher than the Beer-Lambert law limit. When the concentration of a solute is high, the interaction between the solute molecules and the solvent is stronger, causing a different charge distribution on the neighboring species [10]. This will break down the linearity between absorbance and concentration at high concentration. As such, the 20-ppm concentration was found to be the optimum concentration for both MB and MO dyes for UV-visible absorbance data recording and 30 and 40 ppm concentrations were discarded since such values break the linearity of the Beer-Lambert law.

The photodegradation rate of dyes was found to increase as the amount of photocatalysts increase. The amount of ZnO used in this experiment was 10 mg, 20 mg and 30 mg. From Figure 2, 30 mg of ZnO produced the best result because it has a higher catalyst-to-substrate ratio and

more active sites than those of 10 mg and 20 mg. The increase in the number of active sites provides a large surface area for adsorption of dyes and generate more •OH radicals which are responsible for high photocatalytic performance.
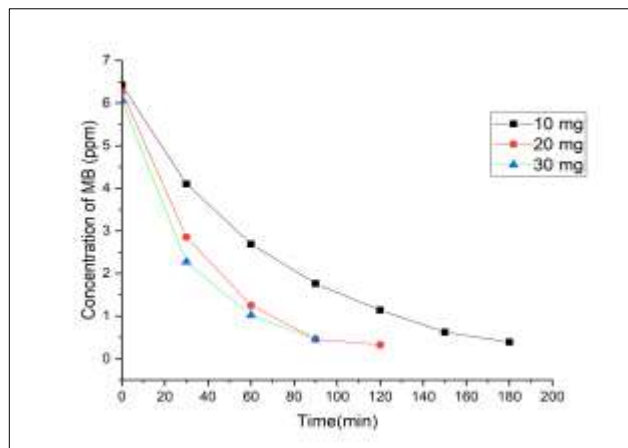

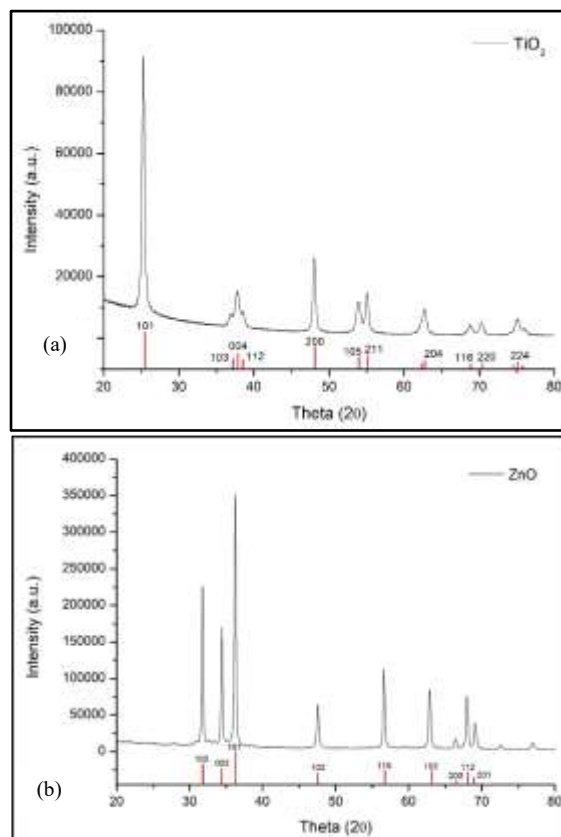Fig. 2 Concentration of MB (ppm) versus Time (min) using ZnO

Fig. 3 XRD pattern for (a) TiO₂ and (b) ZnO

Kinetic studies are presented for MB and MO photodegradation using TiO_2 and ZnO photocatalysts. The order of reaction of MB and MO was found to be first order of reaction kinetics. The calculated rate constant for MB photodegradation from the plot in Figure 4 (a) is 0.0287 s^{-1}. For MO, the rate constant, k is 0.0148 s^{-1}. The order of reaction for both dyes was also found to be first-order of reaction kinetics with MB having a rate constant of 0.0241 s^{-1} and MO having rate constant of 0.0202 s^{-1} [11, 12].

Powder XRD patterns for TiO_2 and ZnO are shown in Figure 3(a) and (b) respectively. The strong diffraction peaks at peak 25.31° and 48.04° confirm the TiO_2 tetragonal anatase structure. There were no spurious diffraction peaks found in the sample, indicating that the TiO_2 contains the anatase structure only and is free from impurities. The XRD pattern of ZnO confirmed that the crystal structure is hexagonal wurtzite. Similar to TiO_2's no other peaks corresponding to impurities were detected in the XRD spectra.

The surface morphology and particle size of TiO_2 and ZnO were imaged using FESEM technique. The statistical evaluation was performed by measuring at least 100 particles from different areas. Figure 4(a) and (b) show the FESEM image of TiO_2 which showed the presence of nanoparticles with average size of 42.5 ± 10.5 nm. Figure 4(c) and (d) show the FESEM image for ZnO which revealed the presence of nanoplates and nanoparticles with average size of 45.2 ± 14.1 nm. The nanoplates structure in ZnO provide a higher surface area when compared to the nanoparticle structure, resulting in a better dye adsorption and providing an interface contact to delay the recombination rate of electron-hole pairs.
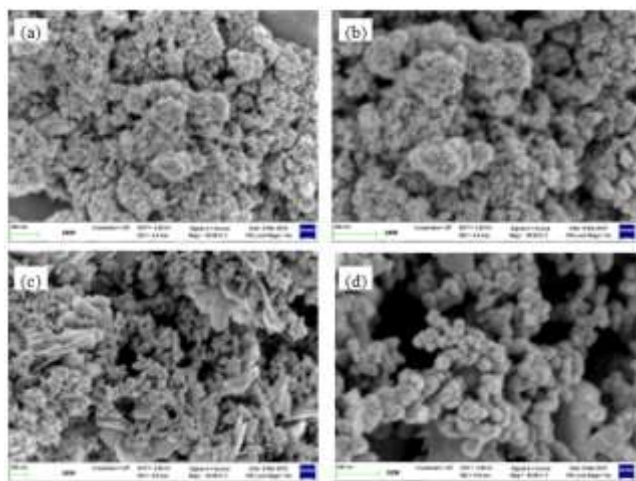

Fig. 4 FESEM images of TiO_2 at (a) low magnification 50 kx, (b) low magnification 80 kx, and ZnO at (c) low magnification 30 kx. (d) high magnification 80 kx

XPS was employed to study the chemical state and elemental composition of photocatalysts. The wide-scan shows no other elemental peaks except Ti 2p, O 1s and C 1s which indicates impurities are absent in the sample (except for the adventitious carbon). The Ti 2p XP spectrum in Figure 5(a) shows a double Ti $2p_{3/2}$ and $2p_{1/2}$ at a separation of 5.7 eV due to the spin-orbit coupling. The Ti $2p_{3/2}$ was found at 458 eV corresponding to the Ti^{4+} state [13]. The O 1s spectrum shown in Figure 5(b) shows a single peak at 529.4 eV which is attributed to the O^{2-} in metal oxides [14]. The XPS results exclude the role of Ti^{3+} sites as photocatalytic active species in this study, contrary to many claims that suggested otherwise [15-17]. Unfortunately, XPS for ZnO cannot be recorded due to limitation of instrumentation. The photon energy needed to record Zn 2p spectrum must be above 1100 eV. However, the instrument that was used only can give 650 eV photon energy.
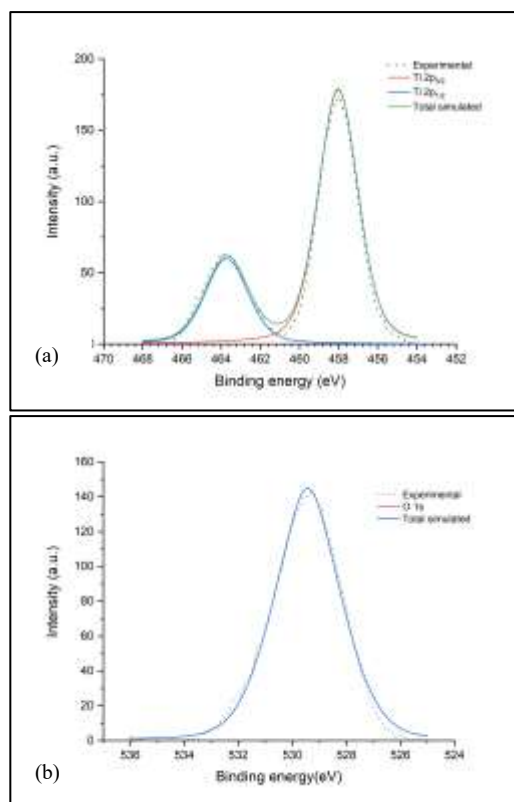

Fig. 5 XP spectra for (a) Ti 2p of TiO_2 and (b) O 1s of TiO

The band gap for TiO_2 and ZnO photocatalysts was determined using a UV-Vis DRS technique. The Kubelka-Munk equation (eqn. 1) is used to convert the reflectance into the absorption coefficient in order to calculate the band gap.

$$\alpha = B \frac{(hv - Eg)^{m/2}}{hv}$$

where α is the absorption coefficient, B is a constant, hv is the energy of the incident radiation, E_g is the energy of the band gap, and m is a constant set to 1 for direct transitions

[18]. The Tauc plot is plotted by using a modified Kubelka-Munk equation, plot of $(\alpha h\nu)^2$ vs $h\nu$, for TiO_2 and ZnO in Figure 6(a) and (b), respectively. The extrapolation of the tangent line of the curve to the energy axis gives the band gap energy. The band gap energy for TiO_2 and ZnO was determined to be 3.46 eV and 3.26 eV, respectively. The slightly lower band gap energy of ZnO than TiO_2 may account for a slightly superior photocatalytic performance of ZnO in both MB and MO photodegradation.
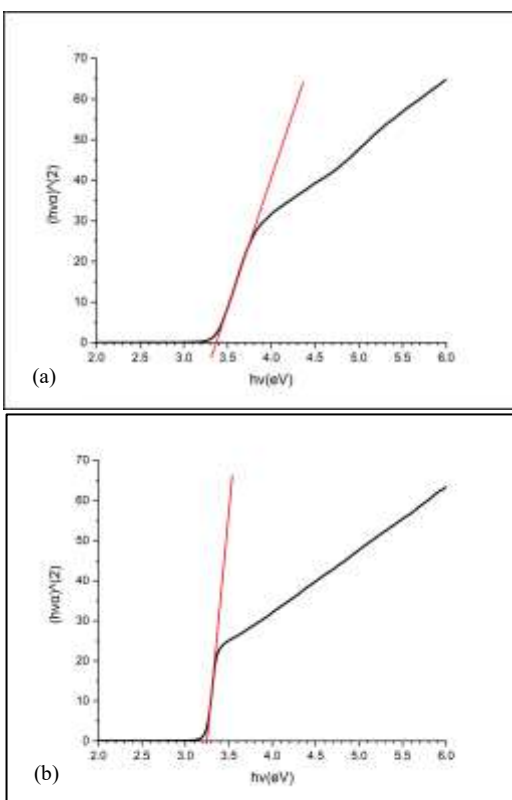

Fig. 6 Tauc plot for band gap determination of (a) TiO_2 and (b) ZnO

4.   CONCLUSION

Photodegradation of dyes, namely methylene blue (MB) and methyl orange (MO) was successfully studied using metal oxide photocatalysts, TiO_2 and ZnO. The factors affecting the photodegradation rate as pH, amount of photocatalysts and concentration of dyes were investigated. ZnO photocatalysts were found to be active in both acidic and basic media for MO and MB degradation. The MB photodegradation rate was found to be the highest when in alkaline condition, consistent with the nature of its cationic dye. For the MO photodegradation, it gave the best result in acidic condition consistent with its characteristic of anionic dye. The XRD data confirmed that TiO_2 has a

tetragonal anatase structure and ZnO has a hexagonal wurtzite structure. FESEM imaging and analysis revealed that the average size for TiO_2 is 42.5 ± 10.5 nm with quasi-spherical nanoparticles and ZnO is 45.2 ± 14.1 nm consisting of nanoplates and nanoparticles. The band gap of TiO_2 and ZnO were measured to be 3.46 and 3.26 eV using a UV-vis DR spectroscopy, respectively. The Ti 2p XP spectrum shows the presence of Ti^{4+} and the O 1s XP spectrum shows the presence of O^{2-} conforming the nature of TiO_2. The XPS results also show no other elemental peaks other than Ti 2p and O 1s indicating that impurities are absent. Overall, ZnO showed a slightly superior photocatalytic performance

REFERENCES

[1] M.M. Khan, S.F. Adil, A. Al-Mayouf, Journal of Saudi Chemical Society, 19 (2015) 462-464.
[2] S.H.S. Chan, T. Yeong Wu, J.C. Juan, C.Y. Teh, Journal of Chemical Technology & Biotechnology, 86 (2011) 1130-1158.
[3] A.B. Djurišić, Y. He, A.M.C. Ng, APL Materials, 8 (2020) 030903.
[4] H. Ji, X. Jing, Y. Xu, J. Yan, H. Li, Y. Li, L. Huang, Q. Zhang, H. Xu, H. Li, RSC Advances, 5 (2015) 57960-57967.
[5] X. Guo, H. Zhu, Q. Li, Applied Catalysis B: Environmental, 160-161 (2014) 408-414.
[6] I.M. Szilágyi, B. Fórizs, O. Rosseler, Á. Szegedi, P. Németh, P. Király, G. Tárkányi, B. Vajna, K. Varga-Josepovits, K. László, A.L. Tóth, P. Baranyai, M. Leskelä, Journal of Catalysis, 294 (2012) 119-127.
[7] M.R.D. Khaki, M.S. Shafeeyan, A.A.A. Raman, W.M.A.W. Daud, Journal of Environmental Management, 198 (2017) 78-94.
[8] D. Matsunami, K. Yamanaka, T. Mizoguchi, K. Kojima, Journal of Photochemistry and Photobiology A: Chemistry, 369 (2019) 106-114.
[9] S. Al-Qaradawi, S.R. Salman, Journal of Photochemistry and Photo biology A: Chemistry, 148 (2002) 161-168.
[10] A.Y. Tolbin, V.E. Pushkarev, L.G. Tomilova, N.S. Zefirov, Physical Chemistry Chemical Physics, 19 (2017) 12953-12958.
[11] M.H. Abdellah, S.A. Nosier, A.H. El-Shazly, A.A. Mubarak, Alexandria Engineering Journal, 57 (2018) 3727-3735.
[12] H.J. Lee, J.H. Kim, S.S. Park, S.S. Hong, G.D. Lee, Journal of Industrial and Engineering Chemistry, 25 (2015) 199-206.
[13] T. Bennett, R.H. Adnan, J.F. Alvino, R. Kler, V.B. Golovko, G.F. Metha, G.G. Andersson, The Journal of Physical Chemistry C, 119 (2015) 11171-11177.
[14] R.H. Adnan, K.L. Woon, N. Chanlek, H. Nakajima, W.H.A. Majid, Australian Journal of Chemistry, 70 (2017) 1110-1117.
[15] Y. Xu, S. Wu, P. Wan, J. Sun, Z.D. Hood, RSC Advances, 7 (2017) 32461-32467.
[16] X. Chen, L. Liu, F. Huang, Chemical Society Reviews, 44 (2015) 1861-1885.
[17] L.R. Grabstanowicz, S. Gao, T. Li, R.M. Rickard, T. Rajh, D.-J. Liu, T. Xu, Inorganic Chemistry, 52 (2013) 3884-3890.
[18] J.-Y. Ruzicka, F. Abu Bakar, C. Hoeck, R. Adnan, C. McNicoll, T.Kemmitt, B.C. Cowie, G.F. Metha, G.G. Andersson, V.B. Golovko, The Journal of Physical Chemistry C, 119 (2015) 24465-24474.